THE JOURNAL OF BIOLOGICAL CHEMISTRY
Vol. 274, No. 25, Issue of June 18, pp. 18135–18139, 1999
© 1999 by The American Society for Biochemistry and Molecular Biology, Inc.
Printed in U.S.A.

Bivalent Inhibitor of the N-end Rule Pathway*

(Received for publication, February 9, 1999)

Yong Tae Kwon‡, Frédéric Lévy§, and Alexander Varshavsky‡¶

From the ‡Division of Biology, California Institute of Technology, Pasadena, California 91125 and the §Ludwig Institute for Cancer Research, 155, ch. Des Boveresses, CH-1066 Epalinges, Switzerland

The N-end rule relates the *in vivo* half-life of a protein to the identity of its N-terminal residue. Ubr1p, the recognition (E3) component of the *Saccharomyces cerevisiae* N-end rule pathway, contains at least two substrate-binding sites. The type 1 site is specific for N-terminal basic residues Arg, Lys, and His. The type 2 site is specific for N-terminal bulky hydrophobic residues Phe, Leu, Trp, Tyr, and Ile. Previous work has shown that dipeptides bearing either type 1 or type 2 N-terminal residues act as weak but specific inhibitors of the N-end rule pathway. We took advantage of the two-site architecture of Ubr1p to explore the feasibility of bivalent N-end rule inhibitors, whose expected higher efficacy would result from higher affinity of the cooperative (bivalent) binding to Ubr1p. The inhibitor comprised mixed tetramers of β-galactosidase that bore *both* N-terminal Arg (type 1 residue) and N-terminal Leu (type 2 residue) but that were resistant to proteolysis *in vivo*. Expression of these constructs in *S. cerevisiae* inhibited the N-end rule pathway much more strongly than the expression of otherwise identical β-galactosidase tetramers whose N-terminal residues were exclusively Arg or exclusively Leu. In addition to demonstrating spatial proximity between the type 1 and type 2 substrate-binding sites of Ubr1p, these results provide a route to high affinity inhibitors of the N-end rule pathway.

Among the targets of the N-end rule pathway are intracellular proteins bearing destabilizing N-terminal residues (1, 2). This proteolytic pathway is one of several pathways of the ubiquitin (Ub)[1] system, whose diverse functions include the regulation of cell growth, division, differentiation, and responses to stress (3–6). Ub is a 76-residue eukaryotic protein that exists in cells either free or conjugated to other proteins. Many of the Ub-dependent regulatory circuits involve processive degradation of ubiquitylated proteins by the 26 S proteasome, an ATP-dependent multisubunit protease (7, 8).

The N-end rule is organized hierarchically. In the yeast *Saccharomyces cerevisiae*, Asn and Gln are tertiary destabilizing N-terminal residues in that they function through their conversion, by the *NTA1*-encoded N-terminal amidase, into the secondary destabilizing N-terminal residues Asp and Glu. The destabilizing activity of N-terminal Asp and Glu requires their conjugation by the *ATE1*-encoded Arg-tRNA-protein transferase (R-transferase) to Arg, one of the primary destabilizing residues (reviewed in Refs. 1 and 9). In mammals, two distinct N-terminal amidases specific, respectively, for N-terminal Asn or Gln mediate the conversion of these tertiary destabilizing residues into the secondary destabilizing residues Asp or Glu (10, 11). The set of secondary destabilizing residues in vertebrates contains not only Asp and Glu but also Cys, which is a stabilizing residue in yeast (9, 12, 13).

The primary destabilizing N-terminal residues are bound directly by N-recognin, the E3 (recognition) component of the N-end rule pathway. In *S. cerevisiae*, N-recognin is the *UBR1*-encoded 225-kDa protein that binds to potential N-end rule substrates through their primary destabilizing N-terminal residues: Phe, Leu, Trp, Tyr, Ile, Arg, Lys, and His (1, 14). The *Ubr1* genes encoding mouse and human N-recognin (also called E3α) have been cloned as well (15). N-recognin has at least two substrate-binding sites. The type 1 site is specific for the basic N-terminal residues Arg, Lys, and His. The type 2 site is specific for the bulky hydrophobic N-terminal residues Phe, Leu, Trp, Tyr, and Ile (1, 12, 16, 17). N-recognin can also target short-lived proteins such as Cup9p (18) and Gpa1p (19, 20), which lack destabilizing N-terminal residues. The Ubr1p-recognized degradation signals of these proteins remain to be characterized in detail.

The known functions of the N-end rule pathway include the control of di- and tripeptide import in *S. cerevisiae* through the degradation of Cup9p, a transcriptional repressor of the peptide transporter gene *PTR2* (18, 21); a mechanistically undefined role in the Sln1p-dependent phosphorylation cascade that mediates osmoregulation in *S. cerevisiae* (22); the degradation of Gpa1p, a Gα protein of *S. cerevisiae* (19, 20); and the conditional degradation of alphaviral RNA polymerase in virus-infected metazoan cells (23). Physiological N-end rule substrates were also identified among the proteins secreted into the cytosol of the host cell by intracellular parasites such as the bacterium *Listeria monocytogenes* (24). Short half-lives of these proteins are required for the efficient presentation of their peptides to the immune system (24). A partial inhibition of the N-end rule pathway was reported to interfere with mammalian cell differentiation (25) and to delay limb regeneration in amphibians (26). Recent evidence suggests that the N-end rule pathway mediates a large fraction of the muscle protein turnover (27) and plays a role in catabolic states that result in muscle atrophy (28).

Targeted mutagenesis has been used to inactivate the N-end rule pathway in *Escherichia coli* and *S. cerevisiae* (14, 29). Analogous mutants have recently been constructed in the mouse as well.[2] These approaches notwithstanding, an efficacious inhibitor of the N-end rule pathway would be useful as well, especially with organisms less tractable genetically. The emerging understanding of the N-end rule pathway in mammals suggests that selective inhibition or activation of this proteolytic system may also have medical applications. Previ-

* This work was supported by National Institutes of Health Grant DK39520 (to A. V.). The costs of publication of this article were defrayed in part by the payment of page charges. This article must therefore be hereby marked "*advertisement*" in accordance with 18 U.S.C. Section 1734 solely to indicate this fact.

¶ To whom correspondence should be addressed: Div. of Biology, 147-75, Caltech, 1200 East California Blvd., Pasadena, CA 91125. Tel.: 626-395-3785; Fax: 626-440-9821; E-mail: avarsh@its.caltech.edu.

[1] The abbreviations used are: Ub, ubiquitin; βgal, *E. coli* β-galactosidase; E3, ubiquitin-protein ligase; ha, hemagglutinin.

[2] Y. T. Kwon and A. Varshavsky, unpublished data.

ous work has shown that millimolar concentrations of amino acid derivatives such as dipeptides bearing destabilizing N-terminal residues can selectively inhibit the N-end rule pathway in extracts from rabbit reticulocytes (12, 17) and *Xenopus* eggs (13), and in intact *S. cerevisiae* cells as well (16). However, the same dipeptides were observed to have at most marginal effects on the N-end rule pathway in intact mammalian cells.[3] One limitation of dipeptide inhibitors is their apparently low affinity for the type 1 and the type 2 site of N-recognin (30).

In the present work, we explored the possibility that a bivalent ligand can bind simultaneously to the type 1 and type 2 sites of N-recognin (see Fig. 1*A*). Similarly to the previously characterized bivalent interactions that involve either macromolecules or small molecules (31, 32), the cooperativity of binding at two independent, mutually nonexclusive sites would be expected to increase the affinity between N-recognin and a bivalent inhibitor by orders of magnitude, in comparison with the affinity of a monovalent binding by the same compound. We show that a bivalent inhibitor of the N-end rule pathway is feasible and consider the implications of this advance.

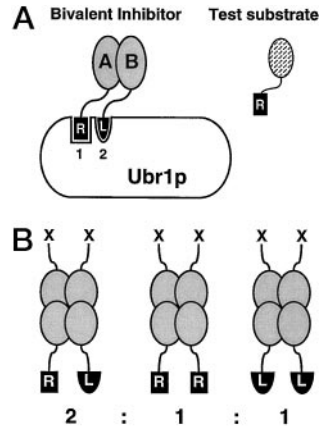

FIG. 1. **The concept of a bivalent inhibitor of the N-end rule pathway.** *A*, the type 1 and type 2 sites of *S. cerevisiae* Ubr1p (N-recognin), which are specific, respectively, for the basic (Arg, Lys, and His) and bulky hydrophobic (Phe, Leu, Trp, Tyr, and Ile) N-terminal residues. In the diagram, the type 1 and type 2 sites are occupied by their ligands, the N-terminal Arg and Leu, borne by a heterodimeric bivalent inhibitor (actually, a tetrameric βgal-based protein in the present work). A test substrate bearing Arg, a type 1 destabilizing N-terminal residue is shown as well. The test substrate, in contrast to the protein-based inhibitor, bears at least one internal Lys residue (not indicated in the diagram) that can function as a component of the N-degron. The type 1 and type 2 sites of N-recognin are shown located close together in the N-terminal region of the 225-kDa Ubr1p. The recent genetic dissection of the Ubr1p substrate-binding sites[6] placed the type 1 and type 2 sites close together in the ~60-kDa N-terminal region of the 225-kDa Ubr1p. *B*, a diagram illustrating the expected frequencies of heterodimeric (Arg- and Leu-bearing) dimers within a βgal-based bivalent inhibitor. Specifically, at equal levels of expression of the two βgal-based polypeptide chains, 50% of βgal tetramers would be expected to be heterotetramers in which at least one of the two dimers bears different (Arg and Leu) N-terminal residues. In the βgal tetramer, the two N termini of each dimer are spatially close, exposed, and oriented in the same direction (40). See also "Results and Discussion."

EXPERIMENTAL PROCEDURES

Strains and General Techniques—The *S. cerevisiae* strains used were JD52 (*MAT**a** ura3-52 his3-Δ200 leu2-3,112 trp1-Δ63 lys2-801*) and JD55 (*MAT**a** ura3-52 his3-Δ200 leu2-3,112 trp1-Δ63 lys2-801 ubr1Δ::HIS3*) (19, 33). Cells were grown on rich (YPD) or synthetic medium containing either 2% dextrose (SD medium), 2% galactose (SG medium), or 2% raffinose (SR medium) (34). To induce the P_{CUP1} promoter, $CuSO_4$ was added to a final concentration of 0.1 mM. Transformation of *S. cerevisiae* was carried out using the lithium acetate method (35).

Plasmids—The high copy (2μ-based) plasmids pRΔ-βgal-TRP1 and pRΔ-βgal-HIS3, which expressed Arg-$e^{\Delta K}$-βgal (Ub-Arg-$e^{\Delta K}$-βgal) (see Fig. 2*A*) from the galactose-inducible $P_{CYC1/GAL1}$ hybrid promoter (2), were produced by replacing the *URA3* marker gene of pFL7 with either *TRP1* or *HIS3*. pLΔ-βgal-TRP1 and pLΔ-βgal-HIS3, both of which expressed Leu-$e^{\Delta K}$-βgal (Ub-Leu-$e^{\Delta K}$-βgal), were produced by replacing the Ub-Arg domain of pRΔ-βgal-TRP1 and pRΔ-βgal-HIS3 with Ub-Leu domain of the pLL2 plasmid.[4] The plasmid pFL7 was produced from pUB23-R (2) by converting the lysine codons 15 and 17 of the extension e^K into arginine codons (36, 37), yielding a construct encoding the extension $e^{\Delta K}$ in front of a βgal moiety lacking the first 23 residues of wild type βgal (see Fig. 2*A*). The low copy, pRS315 vector-derived (38) plasmid pR-eΔKhaUra3-R3R7 expressed Arg-$e^{\Delta K}$-ha-Ura3p^{K3R,K7R} (Ub-Arg-$e^{\Delta K}$-ha-Ura3p^{K3R,K7R}) from the P_{CUP1} promoter. Arg-$e^{\Delta K}$-ha-Ura3p^{K3R,K7R} (see Fig. 2*B*) is called Arg-Ura3p in the main text. In this N-end rule substrate, the residues Lys-3 and Lys-7 of the *S. cerevisiae* Ura3p were converted to arginines (see "Results and Discussion"). In addition, the ha epitope tag (39) was placed between $e^{\Delta K}$ and Ura3p^{K3R,K7R} (see Fig. 2*B*). The plasmid pR-eΔKhaUra3-R3R7 was produced from pFL1 (encoding Ub-Arg-$e^{\Delta K}$-ha-Ura3p) through site-directed mutagenesis of the *URA3* codons for Lys-3 and Lys-7. pFL1 was produced from pKM1235 (which encoded Ub-Arg-e^K-ha-Ura3p)[5] by converting the e^K-coding sequence into the one encoding $e^{\Delta K}$.

Pulse-Chase and Plating Efficiency Assays—Pulse-chase assays with *S. cerevisiae* in mid-exponential growth (A_{600} of ~1) utilized ^{35}S-EXPRESS (NEN Life Science Products) and were carried out as described previously (10, 19), including the immunoprecipitation with anti-βgal and anti-ha antibodies and quantitation with a PhosphorImager (Molecular Dynamics, Sunnyvale, CA). To determine plating efficiency, *S. cerevisiae* strains JD52 (*UBR1*) and JD55 (*ubr1Δ*) expressing Arg-Ura3p (Ub-Arg-$e^{\Delta K}$-ha-Ura3p^{K3R,K7R}; see Fig. 2*B*) were co-transformed with plasmids indicated in the legend to Fig. 3. The transformants were cultured in the raffinose-based medium (SR) lacking Leu, His, and Trp for 20 h. The cultures were then diluted into the otherwise identical galactose-containing (SG) medium to a final A_{600} of 0.1. At an A_{600} of 0.4, cultures were either supplemented with 0.1 mM $CuSO_4$ or left unsupplemented. At the A_{600} of 1.0, the cultures were diluted with SG (which lacks Leu, His, and Trp) either containing or lacking 0.1 mM $CuSO_4$ and were plated on the plates of the same medium composition that also either contained or lacked uracil. The plating efficiency (%) was defined as the ratio of the number of colonies on SG (−Leu, −His, −Trp, −Ura) plates to the number of colonies on SG (−Leu, −His, −Trp) plates, at the same concentration of $CuSO_4$. For each measurement, colonies on 15 plates were counted to yield the average number of colonies per plate.

RESULTS AND DISCUSSION

We constructed a bivalent N-end rule inhibitor (Fig. 1*A*) from the previously studied N-end rule substrates derived from *E. coli* βgal (2). In eukaryotes, linear Ub-protein fusions are rapidly cleaved by deubiquitylating enzymes at the Ub-protein junction, making possible the production of otherwise identical proteins bearing different N-terminal residues, a technical advance that led to the finding of the N-end rule (2). A βgal-based N-end rule substrate contains a destabilizing N-terminal residue (produced *in vivo* using the Ub fusion technique (1)); a ~45-residue, *E. coli* Lac repressor-derived N-terminal extension called e^K (extension *e* bearing lysines *K*); and the βgal moiety lacking its first 21 residues. The resulting X-e^K-βgal is a short-lived protein in both yeast and mammalian cells, whereas an otherwise identical protein bearing a stabilizing N-terminal residue such as Met or Val is metabolically stable (1, 2). An N-degron comprises a destabilizing N-terminal residue and a Lys residue (or residues), the latter being the site of formation of a multi-Ub chain (1, 36). (Ubr1p can also recognize a set of other, internal degrons, which remain to be characterized (18).) If Lys-15 and Lys-17 of the e^K extension are replaced by the Arg residues (which cannot be ubiquitylated), the resulting X-$e^{\Delta K}$-βgal (Fig. 2*A*) is long-lived *in vivo* even if its N-terminal residue is destabilizing in the N-end rule (1, 37).

In the present work, we used the metabolically stable Arg-

[3] F. Lévy and A. Varshavsky, unpublished data.
[4] M. Ghislain and A. Varshavsky, unpublished data.
[5] K. Madura and A. Varshavsky, unpublished data.

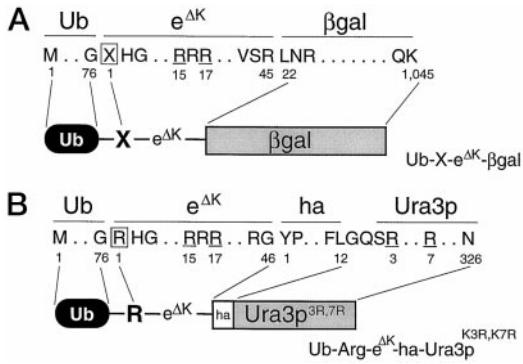

FIG. 2. **Designs of bivalent inhibitor and test substrate.** *A*, the βgal-based fusions (the residue *X* was either Arg or Leu) used to construct the Arg/Leu-bearing bivalent inhibitor. The Ub moiety of the fusions was cotranslationally removed *in vivo* by deubiquitinating enzymes (1). The ~45-residue, *E. coli* Lac repressor-derived sequence termed $e^{\Delta K}$ (extension (*e*) lacking lysines (Δ*K*)), is described in the main text. The βgal part of the fusion lacked the first 21 residues of wild type βgal (2). *B*, the Ura3p-based N-end rule substrate, Arg-$e^{\Delta K}$-ha-$Ura3p^{K3R,K7R}$, derived from Ub-Arg-$e^{\Delta K}$-ha-$Ura3p^{K3R,K7R}$ and denoted Arg-Ura3p, is described in the main text.

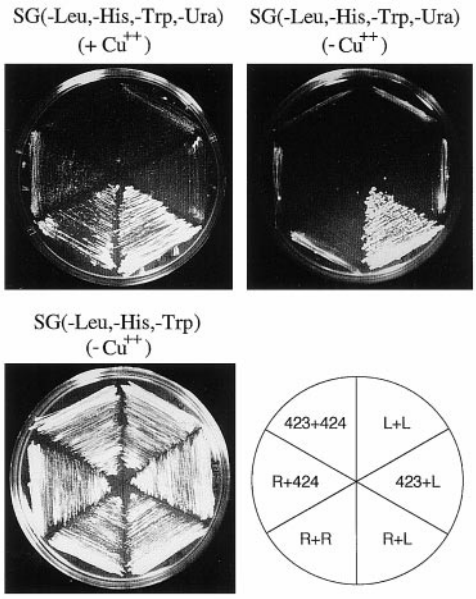

FIG. 3. **A bivalent, but not monovalent, inhibitor of Ubr1p confers Ura$^+$ phenotype on cells expressing the short-lived N-end rule substrate Arg-Ura3p.** *S. cerevisiae* JD52 (*UBR1*) expressing Arg-Ura3p (Ub-Arg-Ura3p), a short-lived reporter (Fig. 2B), were cotransformed, alternatively, with pRS423 (*HIS3*-based control vector) and pRS424 (P_{GAL1}, *TRP1*-based control vector) (denoted as *423+424*); with pRS424 and pRΔ-βgal-HIS3, expressing Arg-$e^{\Delta K}$-βgal (Ub-Arg-$e^{\Delta K}$-βgal) (denoted as *R+424*; monovalent inhibitor); with pRS423 and pLΔ-βgal-TRP1, expressing Leu-$e^{\Delta K}$-βgal (Ub-Leu-$e^{\Delta K}$-βgal) (denoted as *423+L*); with pRΔ-βgal-HIS3 and pRΔ-βgal-TRP1, both expressing Arg-$e^{\Delta K}$-βgal (denoted as *R+R*; monovalent inhibitor); with pLΔ-βgal-HIS3 and pLΔ-βgal-TRP1, both expressing Leu-$e^{\Delta K}$-βgal (denoted as *L+L)*; or with pRΔ-βgal-HIS3 and pLΔ-βgal-TRP1, expressing Arg-$e^{\Delta K}$-βgal and Leu-$e^{\Delta K}$-βgal (denoted as *R+L*; the bivalent inhibitor). Cells were streaked on SG medium containing 0.1 mM $CuSO_4$ and lacking Leu, His, Trp, and Ura (*upper left panel*), on the otherwise identical medium lacking the added $CuSO_4$ (*upper right panel*), or on the Ura-containing SG medium lacking Leu, His, and Trp (controls; *lower left panel*). Plates were incubated at 30 °C for 3 days.

$e^{\Delta K}$-βgal (produced from Ub-Arg-$e^{\Delta K}$-βgal) and Leu-$e^{\Delta K}$-βgal (produced from Ub-Leu-$e^{\Delta K}$-βgal). These proteins retain the ability to bind, respectively, to the type 1 and type 2 sites of N-recognin but cannot be ubiquitylated (37), apparently because the most N-terminal Lys residue in X-$e^{\Delta K}$-βgal, at position 239, is too far from the N terminus of the protein. In the βgal tetramer, the two N termini of each dimer are spatially close, exposed, and oriented in the same direction (40). At equal levels of expression of the two βgal-based polypeptide chains such as Arg-$e^{\Delta K}$-βgal and Leu-$e^{\Delta K}$-βgal, 50% of βgal tetramers would be expected to be heterotetramers in which at least one of the two dimers bears different (Arg and Leu) N-terminal residues (Fig. 1*B*). If the type 1 and type 2 substrate-binding sites of the 225-kDa Ubr1p are appropriately located and oriented, they might be able to bind the Arg- and Leu-bearing subunits of the mixed βgal tetramer, especially in view of the presumed flexibility of the $e^{\Delta K}$ extension (1) (Fig. 1*A*).

The reporter N-end rule substrate in this study was Arg-$e^{\Delta K}$-ha-$Ura3p^{K3R,K7R}$, denoted below as Arg-Ura3p (Fig. 2*B*). This ha-tagged, type 1 N-end rule substrate was produced from Ub-Arg-$e^{\Delta K}$-ha-$Ura3p^{K3R,K7R}$ through the cotranslational *in vivo* cleavage by deubiquitinating enzymes (1, 6, 41). The lysine-lacking $e^{\Delta K}$ extension of Arg-$e^{\Delta K}$-ha-$Ura3p^{K3R,K7R}$, and the replacement of the first two lysines of the Ura3p moiety with arginines were used to decrease the rate of degradation of Arg-Ura3p by the N-end rule pathway and also to reduce the slow but detectable degradation of Arg-Ura3p by yet another pathway, through a degron distinct from the N-degron.[3] Several Lys residues of Ura3p other than Lys-3 and Lys-7 are also close to its N terminus, thus accounting for the absence, in this case, of the all-or-none effect on the reporter degradation that is observed when e^K is replaced with $e^{\Delta K}$ in an X-e^K-βgal substrate (37). The Lys-3 → Arg and Lys-7 → Arg modifications decreased the enzymatic activity of the Ura3p moiety.[2] The reduced enzymatic activity of $Ura3p^{K3R,K7R}$ facilitated selection assays (Figs. 3 and 4).

The first bivalent inhibitor assay employed *ura3 S. cerevisiae* expressing Arg-Ura3p (Fig. 2*B*) from the uninduced P_{CUP1} promoter. The Ubr1p-mediated degradation of Arg-Ura3p ($t_{½}$ of ~8 min) and its correspondingly low steady-state concentration rendered wild type (*UBR1*) cells phenotypically Ura$^-$, whereas *ubr1*Δ strains expressing Arg-Ura3p were phenotypically Ura$^+$ (Figs. 3 and 4 and data not shown). Cells expressing Arg-Ura3p were cotransformed with two control plasmids (vectors; *423+424* in Fig. 3). Alternatively, these cells were cotransformed with two plasmids (bearing different selectable markers) that expressed either Arg-$e^{\Delta K}$-βgal alone (*R+R* in Fig. 3), Leu-$e^{\Delta K}$-βgal alone (*L+L* in Fig. 3), or both of them together (*R+L* in Fig. 3; the bivalent inhibitor mode) from a galactose-inducible promoter. Pairs of alternatively marked plasmids were used to make certain that the conditions of expression and the total amounts of βgal-based proteins produced remained the same in all of these settings. The transformants were streaked on SG medium lacking uracil.

Remarkably, only those Arg-Ura3p-expressing cells that expressed *both* Arg-$e^{\Delta K}$-βgal and Leu-$e^{\Delta K}$-βgal became Ura$^+$ under these conditions (Fig. 3). The cells that expressed either Arg-$e^{\Delta K}$-βgal alone or Leu-$e^{\Delta K}$-βgal alone remained Ura$^-$, as did the cells that received control plasmids (Fig. 3). (The same cells grew equally well in the control SG medium containing uracil (Fig. 3, *bottom left panel*).) Note that the monovalent inhibitors were ineffective despite the fact that the concentration of either the Arg-based N terminus alone or the Leu-based N terminus alone was twice the concentration of the same N termini in the case of the bivalent inhibitor.

To quantify the effect of coexpressing Arg-$e^{\Delta K}$-βgal and Leu-$e^{\Delta K}$-βgal on the rescue of the Ura$^+$ phenotype, a plating efficiency assay was carried out with the same transformants. Equal amounts of cells were plated on SG(+Ura) and SG(−Ura) plates, and the numbers of colonies were determined. When the Arg-Ura3p reporter was expressed at a sufficiently low rate (uninduced P_{CUP1} promoter), cells became

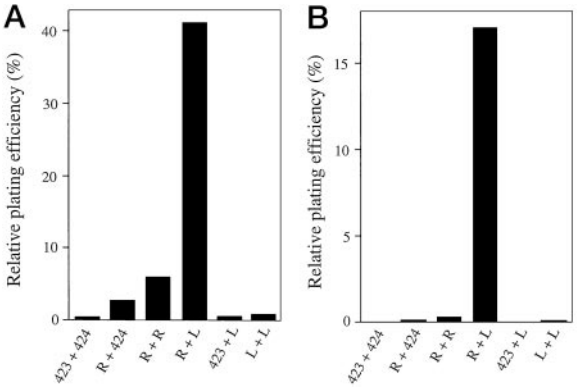

FIG. 4. **Plating efficiencies of *S. cerevisiae* expressing Arg-Ura3p in the presence of bivalent and monovalent inhibitors of the N-end rule pathway.** *A*, *S. cerevisiae* JD52 (*UBR1*) and JD55 (*ubr1*Δ) expressing Arg-Ura3p were cotransformed with the sets of plasmids described and denoted in the legend to Fig. 3. The transformants were cultured as described under "Experimental Procedures" and plated on either SG(−Leu, −His, −Trp, −Ura) plates or control plates SG(−Leu, −His, −Trp) containing 0.1 mM $CuSO_4$. The plating efficiencies shown are the values produced by normalization against the absolute plating efficiency (92%) of the positive control: the *ubr1*Δ strain JD55 expressing Arg-Ura3p and bearing the vector pRS424. *B*, the same experiment was done using plates lacking the added $CuSO_4$. The plating efficiencies shown are the values produced by normalization against the positive control used in *A*. Under these growth conditions (no added $CuSO_4$), the absolute plating efficiency of the positive control was 26%.

Ura$^+$ (through metabolic stabilization of Arg-Ura3p) only in the presence of *both* Arg-e$^{\Delta K}$-βgal and Leu-e$^{\Delta K}$-βgal (Fig. 4*B*). A weak stabilizing effect of Arg-e$^{\Delta K}$-βgal alone could be detected only at a ~20-fold higher level of Arg-Ura3p expression (induced P_{CUP1} promoter) (Fig. 4*A*). No stabilization of Arg-Ura3p was observed in the presence of Leu-e$^{\Delta K}$-βgal under any conditions (Fig. 4), confirming the specificity of inhibition in regard to the type (basic or bulky hydrophobic) of the primary destabilizing N-terminal residue of the reporter. Higher sensitivity of this assay at the higher level of Arg-Ura3p expression results from a higher steady-state level of the short-lived Arg-Ura3p, so that even its marginal stabilization suffices to render a small fraction of cells Ura$^+$ (Fig. 4*A*; compare with Fig. 4*B*).

To analyze directly the *in vivo* degradation of Arg-Ura3p in the presence of different combinations of X-e$^{\Delta K}$-βgal proteins, the transformants of Figs. 3 and 4 were subjected to pulse-chase analysis, with immunoprecipitation of both Arg-Ura3p and the (long-lived) X-e$^{\Delta K}$-βgals (Fig. 5). Quantitation of the resulting electrophoretic patterns (Fig. 5*C*) confirmed and extended the conclusions reached through phenotypic analyses (Figs. 3 and 4). Specifically, the normally short-lived Arg-Ura3p (Fig. 5*A*, *lanes 1–3*) was strongly (but still incompletely) stabilized in the presence of both Arg-e$^{\Delta K}$-βgal and Leu-e$^{\Delta K}$-βgal (Fig. 5*A*, *lanes 4–6*; compare with *lanes 1–3* and *7–9*). This stabilization was manifested especially clearly as an increase in the relative amount of Arg-Ura3p at the beginning of chase (time 0), indicating reduced degradation of Arg-Ura3p during the pulse (Fig. 5*C*). This latter degradation pattern, termed "zero point effect," is caused by the previously demonstrated preferential targeting of newly formed (as distinguished from conformationally mature) protein substrates by the N-end rule pathway (16, 42). The increased steady-state level of Arg-Ura3p in the presence of both Arg-e$^{\Delta K}$-βgal and Leu-e$^{\Delta K}$-βgal accounted for the results of phenotypic analyses (Figs. 3 and 4). The much smaller but detectable stabilization of Arg-Ura3p by Arg-e$^{\Delta K}$-βgal alone (Fig. 5*C*) was consistent not only with the inability of Arg-e$^{\Delta K}$-βgal to confer the Ura$^+$ phenotype on cells expressing Arg-Ura3p from uninduced P_{CUP1} promoter but also with the partial rescue of the Ura$^+$ phenotype by Arg-e$^{\Delta K}$-βgal in cells expressing Arg-Ura3p from the induced P_{CUP1} (Figs. 3 and 4 and data not shown).

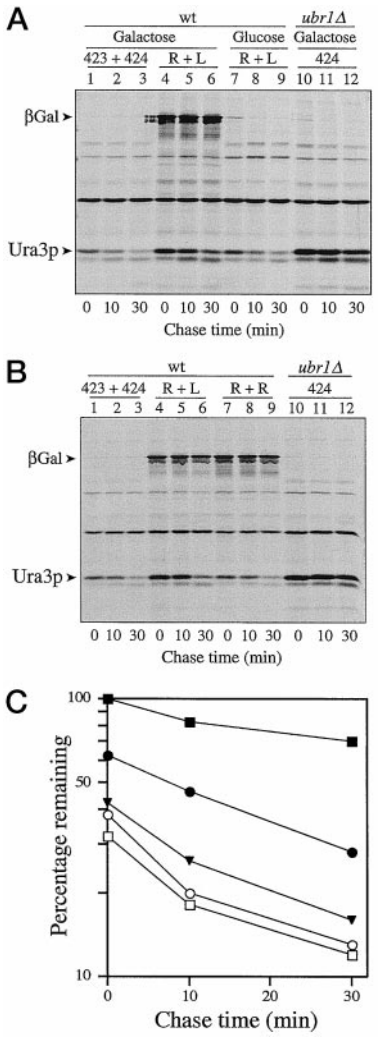

FIG. 5. **Metabolic stabilization of Arg-Ura3p in the presence of bivalent N-end rule inhibitor.** *A*, *S. cerevisiae* JD52 (*UBR1*) expressing Arg-Ura3p, a short-lived Ura3p-based reporter (Fig. 2*B*), from the induced P_{CUP1} promoter, were cotransformed, alternatively, with either pRS423 (*HIS3*-based control vector) and pRS424 (P_{GAL1}, *TRP1*-based control vector) (denoted as *423+424*), or with pRΔ-βgal-TRP1 and pLΔ-βgal-HIS3, expressing Arg-e$^{\Delta K}$-βgal and Leu-e$^{\Delta K}$-βgal (denoted as *R+L*; the bivalent inhibitor). Control JD55 (*ubr1*Δ) cells expressing Arg-Ura3p were transformed with pRS424. Cells grown in either dextrose-containing SD medium (no expression of βgal) or galactose-containing SG medium were labeled with [^{35}S]methionine/cysteine for 5 min at 30 °C, followed by a chase for 0, 10, and 30 min, extraction, immunoprecipitation, and SDS-10% polyacrylamide gel electrophoresis. *B*, same as in *A*, but cells were also cotransformed with the plasmids pRΔ-βgal-TRP1 and pRΔ-βgal-HIS3, both expressing Arg-eΔK-βgal (denoted as *R+R*). The assays were carried out in SG medium. *C*, *in vivo* decay curves of Arg-Ura3p (Fig. 2*B*) in wild type (JD52) and *ubr1*Δ (JD55) cells. The patterns in *A* and *B* were quantified as described under "Experimental Procedures." The initial amounts of Arg-Ura3p were normalized against the amount in *ubr1*Δ cells (100%). Note that the inhibitors also altered the zero point effect (degradation of a reporter *during* the pulse (16, 42)). ●, degradation of Arg-Ura3p in *UBR1* (JD52) cells in the presence of both Arg-e$^{\Delta K}$-βgal and Leu-e$^{\Delta K}$-βgal (cells were grown in SG medium); ○, the same transformants were grown in SD medium where βgal fusions were not expressed; ▼, JD52 cells expressing Arg-Ura3p were transformed with the two alternatively marked plasmids expressing Arg-e$^{\Delta K}$-βgal and grown in SG medium; □, JD52 cells expressing Arg-Ura3p were transformed with the two alternatively marked control vectors and grown in SG medium; ■, *ubr1*Δ (JD55) cells expressing Arg-Ura3p were transformed with control vectors and grown in SG medium.

The Arg/Leu-e$^{\Delta K}$-βgal-based bivalent inhibitor of the present work, although surprisingly potent (Fig. 4*B*), is obviously far from optimal even for a protein-based inhibitor; because βgal is a homotetramer, only ~50% of the coexpressed Arg-e$^{\Delta K}$-βgal and Leu-e$^{\Delta K}$-βgal chains would exist as heterodimers within tetramers (Fig. 1*B*). (This estimate assumes a random assortment of Arg- and Leu-bearing βgal chains in the formation of βgal tetramers. The actual *in vivo* assortment is expected to be biased, to an unknown extent, in favor of homodimeric associations, because individual polysomes would produce βgal chains bearing either Arg or Leu but not both.) In addition, although the e$^{\Delta K}$ extension (Fig. 2*A*) is capable of supporting the desired effects, it is also unlikely to be optimal. In summary, the efficacy of this first and necessarily suboptimal bivalent inhibitor bodes well for the future of this design.

A bivalent inhibitor is strikingly more efficacious than an otherwise identical monovalent inhibitor (Figs. 3–5). In addition, our findings are the first evidence that the type 1 and type 2 sites of N-recognin are spatially proximal in the 225-kDa *S. cerevisiae* Ubr1p. While this work was under way, genetic dissection of *S. cerevisiae* Ubr1p identified amino acid residues that are required for the integrity of the type 1 site but not the type 2 site, and *vice versa*.[6] These results provided independent evidence for both the separateness and spatial proximity of the two substrate-binding sites of the 225-kDa N-recognin, in agreement with the present data. Our results (Figs. 3–5) strongly suggest that small bivalent inhibitors of the N-end rule pathway are feasible, and moreover, are expected to be much more potent than their monovalent counterparts. Work to produce such inhibitors is under way.

Acknowledgments—We thank members of the Varshavsky laboratory, especially A. Kashina and G. Turner, for helpful discussions and advice in the course of this work. We also thank I. Davydov, F. Du, F. Navarro-Garcia, H. Rao, and especially G. Turner for comments on the manuscript.

REFERENCES

1. Varshavsky, A. (1996) *Proc. Natl. Acad. Sci. U. S. A.* **93,** 12142–12149
2. Bachmair, A., Finley, D., and Varshavsky, A. (1986) *Science* **234,** 179–186
3. Hershko, A. (1991) *Trends Biochem. Sci.* **16,** 265–268
4. Peters, J.-M., King, R. W., and Deshaies, R. J. (1998) in *Ubiquitin and the Biology of the Cell*, pp. 345–387, Plenum Press, New York
5. Varshavsky, A. (1997) *Trends Biochem. Sci.* **22,** 383–387
6. Hochstrasser, M. (1996) *Annu. Rev. Genet.* **30,** 405–439
7. Baumeister, W., Walz, J., Zühl, F., and Seemüller, E. (1998) *Cell* **92,** 367–380
8. Rechsteiner, M. (1998) in *Ubiquitin and the Biology of the Cell* (Peters, J. M., Harris, J. R., and Finley, D., eds) pp. 147–189, Plenum Press, New York
9. Kwon, Y. T., Kashina, A. S., and Varshavsky, A. (1999) *Mol. Cell. Biol.* **19,** 182–193
10. Grigoryev, S., Stewart, A. E., Kwon, Y. T., Arfin, S. M., Bradshaw, R. A., Jenkins, N. A., Copeland, N. G., and Varshavsky, A. (1996) *J. Biol. Chem.* **271,** 28521–28532
11. Stewart, A. E., Arfin, S. M., and Bradshaw, R. A. (1995) *J. Biol. Chem.* **270,** 25–28
12. Gonda, D. K., Bachmair, A., Wünning, I., Tobias, J. W., Lane, W. S., and Varshavsky, A. (1989) *J. Biol. Chem.* **264,** 16700–16712
13. Davydov, I. V., Patra, D., and Varshavsky, A. (1998) *Arch. Biochem. Biophys.* **357,** 317–325
14. Bartel, B., Wünning, I., and Varshavsky, A. (1990) *EMBO J.* **9,** 3179–3189
15. Kwon, Y. T., Reiss, Y., Fried, V. A., Hershko, A., Yoon, J. K., Gonda, D. K., Sangan, P., Copeland, N. G., Jenkins, N. A., and Varshavsky, A. (1998) *Proc. Natl. Acad. Sci. U. S. A.* **95,** 7898–7903
16. Baker, R. T., and Varshavsky, A. (1991) *Proc. Natl. Acad. Sci. U. S. A.* **87,** 2374–2378
17. Reiss, Y., Kaim, D., and Hershko, A. (1988) *J. Biol. Chem.* **263,** 2693–2269
18. Byrd, C., Turner, G. C., and Varshavsky, A. (1998) *EMBO J.* **17,** 269–277
19. Madura, K., and Varshavsky, A. (1994) *Science* **265,** 1454–1458
20. Schauber, C., Chen, L., Tongaonkar, P., Vega, I., and Madura, K. (1998) *Genes Cells* **3,** 307–319
21. Alagramam, K., Naider, F., and Becker, J. M. (1995) *Mol. Microbiol.* **15,** 225–234
22. Ota, I. M., and Varshavsky, A. (1993) *Science* **262,** 566–569
23. deGroot, R. J., Rümenapf, T., Kuhn, R. J., and Strauss, J. H. (1991) *Proc. Natl. Acad. Sci. U. S. A.* **88,** 8967–8971
24. Sijts, A. J., Pilip, I., and Pamer, E. G. (1997) *J. Biol. Chem.* **272,** 19261–19268
25. Hondermarck, H., Sy, J., Bradshaw, R. A., and Arfin, S. M. (1992) *Biochem. Biophys. Res. Commun.* **30,** 280–288
26. Taban, C. H., Hondermarck, H., Bradshaw, R. A., and Boilly, B. (1996) *Experientia* **52,** 865–870
27. Solomon, V., Lecker, S. H., and Goldberg, A. L. (1998) *J. Biol. Chem.* **273,** 25216–25222
28. Solomon, V., Baracos, V., Sarraf, P., and Goldberg, A. (1998) *Proc. Natl. Acad. Sci. U. S. A.* **95,** 12602–12607
29. Tobias, J. W., Shrader, T. E., Rocap, G., and Varshavsky, A. (1991) *Science* **254,** 1374–1377
30. Varshavsky, A., Byrd, C., Davydov, I. V., Dohmen, R. J., Du, F., Ghislain, M., Gonzalez, M., Grigoryev, S., Johnson, E. S., Johnsson, N., Johnston, J. A., Kwon, Y. T., Lévy, F., Lomovskaya, O., Madura, K., Ota, I., Rümenapf, T., Shrader, T. E., Suzuki, T., Turner, G., Waller, P. R. H., and Webster, A. (1998) in *Ubiquitin and the Biology of the Cell* (Peters, J.-M., Harris, J. R., and Finley, D., eds) pp. 223–278, Plenum Press, New York
31. Kramer, R. H., and Karpen, J. W. (1998) *Nature* **395,** 710–713
32. Ptashne, M. (1992) *A Genetic Switch*, Cell Press, Cambridge, MA
33. Madura, K., Dohmen, R. J., and Varshavsky, A. (1993) *J. Biol. Chem.* **268,** 12046–12054
34. Sherman, F. (1991) *Methods Enzymol.* **194,** 3–21
35. Ausubel, F. M., Brent, R., Kingston, R. E., Moore, D. D., Smith, J. A., Seidman, J. G., and Struhl, K. (eds) (1996) *Current Protocols in Molecular Biology*, Wiley-Interscience, New York
36. Bachmair, A., and Varshavsky, A. (1989) *Cell* **56,** 1019–1032
37. Johnson, E. S., Gonda, D. K., and Varshavsky, A. (1990) *Nature* **346,** 287–291
38. Sikorski, R. S., and Hieter, P. (1989) *Genetics* **122,** 19–27
39. Johnson, E. S., Ma, P. C., Ota, I. M., and Varshavsky, A. (1995) *J. Biol. Chem.* **270,** 17442–17456
40. Jacobson, R. H., Zhang, X. J., DuBose, R. F., and Matthews, B. W. (1994) *Nature* **369,** 761–766
41. Ghislain, M., Dohmen, R. J., Levy, F., and Varshavsky, A. (1996) *EMBO J.* **15,** 4884–4899
42. Lévy, F., Johnsson, N., Rümenapf, T., and Varshavsky, A. (1996) *Proc. Natl. Acad. Sci. U. S. A.* **93,** 4907–4912

[6] A. Webster, M. Ghislain, and A. Varshavsky, unpublished data.